



Late Holocene Landscape Collapse of a Trans-Himalayan Dryland: Human Impact and Aridification

Johanna Menges, Niels Hovius, Christoff Andermann, Michael Dietze, Charlie Swoboda, Kristen L. Cook, Basanta R. Adhikari, Andrea Vieth-Hillebrand, Stephane Bonnet, Tony Reimann, et al.

► To cite this version:

Johanna Menges, Niels Hovius, Christoff Andermann, Michael Dietze, Charlie Swoboda, et al.. Late Holocene Landscape Collapse of a Trans-Himalayan Dryland: Human Impact and Aridification. *Geophysical Research Letters*, 2019, 46, pp.13,814-13,824. 10.1029/2019GL084192 . insu-03661409

HAL Id: insu-03661409

<https://insu.hal.science/insu-03661409>

Submitted on 7 May 2022

HAL is a multi-disciplinary open access archive for the deposit and dissemination of scientific research documents, whether they are published or not. The documents may come from teaching and research institutions in France or abroad, or from public or private research centers.

L'archive ouverte pluridisciplinaire **HAL**, est destinée au dépôt et à la diffusion de documents scientifiques de niveau recherche, publiés ou non, émanant des établissements d'enseignement et de recherche français ou étrangers, des laboratoires publics ou privés.



Distributed under a Creative Commons Attribution 4.0 International License

Geophysical Research Letters

RESEARCH LETTER

10.1029/2019GL084192

Key Points:

- We document an eco-geomorphic tipping point, plunging a landscape at the southern edge of the Tibetan plateau into an erosional state
- The tipping point occurred 1.6 ka ago, it was facilitated by a period of human land use and triggered by late Holocene aridification
- At sustained modern erosion rates of 1 mm/year, soils are removed on a millennial time scale, precluding fast recovery of the landscape

Supporting Information:

- Supporting Information S1

Correspondence to:

J. Menges,
menges@gfz-potsdam.de

Citation:

Menges, J., Hovius, N., Andermann, C., Dietze, M., Swoboda, C., Cook, K. L., et al. (2019). Late Holocene landscape collapse of a trans-Himalayan dryland: Human impact and aridification. *Geophysical Research Letters*, 46, 13,814–13,824. <https://doi.org/10.1029/2019GL084192>

Received 20 JUN 2019

Accepted 9 NOV 2019

Accepted article online 3 DEC 2019

Published online 10 DEC 2019

Late Holocene Landscape Collapse of a Trans-Himalayan Dryland: Human Impact and Aridification

Johanna Menges¹ , Niels Hovius^{1,2} , Christoff Andermann¹ , Michael Dietze¹ , Charlie Swoboda², Kristen L. Cook¹, Basanta R. Adhikari³, Andrea Vieth-Hillebrand⁴ , Stephane Bonnet⁵ , Tony Reimann⁶, Andreas Koutsodendris⁷ , and Dirk Sachse¹ 

¹Section 4.6, GFZ German Research Centre for Geosciences, Potsdam, Germany, ²Institute of Geosciences, University of Potsdam, Potsdam-Golm, Germany, ³Department of Civil Engineering, Institute of Engineering, Tribhuvan University, Kirtipur, Nepal, ⁴Section 3.2, GFZ German Research Centre for Geosciences, Potsdam, Germany, ⁵GET CNRS Univ Toulouse, UMR 5563, 14, Avenue Édouard Belin, Toulouse, France, ⁶Soil Geography and Landscape group & Netherlands Centre for Luminescence dating, Wageningen University, Wageningen, The Netherlands, ⁷Institute of Earth Sciences, Heidelberg University, Heidelberg, Germany

Abstract Soil degradation is a severe and growing threat to ecosystem services globally. Soil loss is often nonlinear, involving a rapid deterioration from a stable eco-geomorphic state once a tipping point is reached. Soil loss thresholds have been studied at plot scale, but for landscapes, quantitative constraints on the necessary and sufficient conditions for tipping points are rare. Here, we document a landscape-wide eco-geomorphic tipping point at the edge of the Tibetan Plateau and quantify its drivers and erosional consequences. We show that in the upper Kali Gandaki valley, Nepal, soil formation prevailed under wetter conditions during much of the Holocene. Our data suggest that after a period of human pressure and declining vegetation cover, a 20% reduction of relative humidity and precipitation below 200 mm/year halted soil formation after 1.6 ka and promoted widespread gullyling and rapid soil loss, with irreversible consequences for ecosystem services.

Plain Language Summary Two billion people live in drylands, where small changes in climate and land use can have large impacts on soil stability and food security. It is important to know the thresholds of eco-geomorphic stability in such settings. Here, we determine the conditions that tipped a trans-Himalayan dryland into irreversible degradation. We show that in the upper Kali Gandaki valley, Nepal, sustained soil formation terminated after 1.6 ka. Human pressure in the preceding period had reduced vegetation cover, but a 20% drop in relative humidity and a precipitation decrease to below 200 mm/year promoted widespread, rapid badland formation. These values may serve as indicators elsewhere, but local eco-geomorphic threshold values are likely to differ between landscapes due to other essential variables.

1. Introduction

Human activity and climate variations are principal drivers of land degradation in dry regions (UNCCD, 1994). They can push fragile landscapes into a state where soils are lost and ecosystems cease to sustain the production of food, fodder, and fuel (Millennium Ecosystem Assessment, 2005). These effects may be amplified by positive feedbacks limiting the chance of recovery (D'Odorico et al., 2013; Scheffer et al., 2001). Anticipation and mitigation of eco-geomorphic tipping points are limited by imperfect knowledge of the evolving conditions of coupled human-environmental systems and their nonlinear dynamics (Reynolds et al., 2007). Most important, we must know the necessary and sufficient conditions for system collapse. Past tipping points can yield critical insights and help constrain the sensitivity of fragile drylands to current and future stresses.

High elevation drylands, such as those in Tibet and the rain shadow of the Himalayas, are particularly vulnerable landscapes, affected by desertification and loss of ecosystem services (Cui & Graf, 2009). With the earliest permanent presence of humans in central Tibet dated to 8 ka (Meyer et al., 2017), a significant human impact on the vegetation cover since the mid-Holocene has been suggested (Miehe et al., 2014). In parallel, climate change is seen as a driver of vegetation changes (Shen et al., 2008). The relative importance and interplay of these forcing mechanisms remains unknown. Valleys traversing the Himalayas at the

©2019. The Authors.

This is an open access article under the terms of the Creative Commons Attribution License, which permits use, distribution and reproduction in any medium, provided the original work is properly cited.

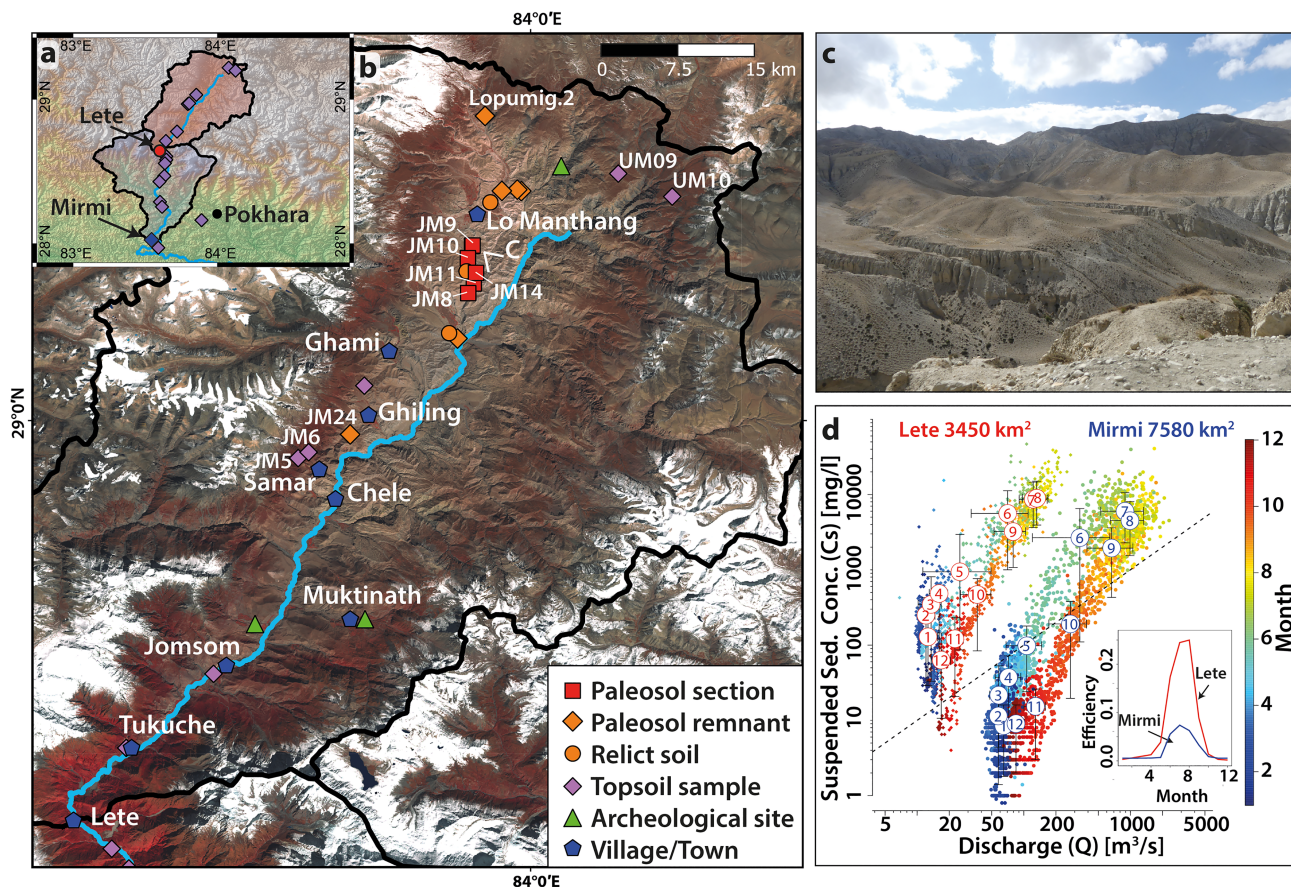


Figure 1. Overview of study area. (a) Map showing upper (N of Lete) and lower (N of Mirmi) KG catchment and sampled modern soils (diamonds). (b) Color infrared Landsat 8 image of the upper KG valley, with sample locations: paleosol sections (red), soil remnants (orange), modern soils (violet), archeological sites (green), and villages (blue). (c) Photograph looking SE showing the preexisting smooth landscape in the back with active gullies, disconnected from a large canyon associated with retrogressive erosion of the KG River. (d) Plot of suspended sediment concentration against daily river discharge measured at Lete (red) 2011 to 2012 and 2015 to 2016 and Mirmi (blue) 2006 to 2015. Point color indicates time of year, numbered open circles are monthly mean values, and whiskers 10% and 90% quantiles. (inset) Monthly bulk erosion efficiency calculated as the ratio of suspended sediment yield ($t/km^2/day$) and runoff per unit area (mm/day).

southern edge of the Tibetan Plateau have strong climatic gradients and a history of human settlement, making them ideally suited to exploring the combined effects of human and climatic landscape disturbance.

Here, we focus on the upper Kali Gandaki (KG) valley, where modern erosion rates are high. We show that its landscape was in a geomorphologically stable state supporting soils and vegetation during much of the Holocene. We determine the timing of the transition between these two states and explore the roles of human land use and hydroclimatic change, combining archeological data with a new hydroclimate record of biomarker and compound-specific stable isotopes in paleosols.

2. Materials and Methods

2.1. Study Area

The KG valley in central Nepal (Figures 1a and 1b) connects headwaters north of the High Himalayan summits of Dhaulagiri and Annapurna to the Gangetic plains in the south. In the headwaters, a gently sloping open mountain region with elevations of up to 6 km hosts an incised channel network that has been expanding northward on million-year time scales (Fort et al., 1982). This part of the KG catchment is located in poorly consolidated clastic sediments of the Neogene Thakkola formation and Pleistocene valley fills (Adhikari & Wagreich, 2011). Downstream, the river enters the High Himalayas transitioning into a steep and deeply incised valley at Lete (~2,500 m asl.). This valley has been a corridor for trade between Tibet and India at least since 3 ka (Aldenderfer & Eng, 2016; Simons et al., 1994). In this region, topographic

blocking of the Indian Summer Monsoon (ISM) causes a pronounced precipitation gradient (Bookhagen & Burbank, 2010), dropping from over 2,000 mm/year at the orographic barrier to 160 mm/year in the upper KG valley to the north (Garzione et al., 2000). Local biomes are adapted to this climate gradient, dense mountain forests in the High Himalayas grading into sparse dwarf shrubs in the upper valley drylands (Kriechbaum, 2002; Miehe et al., 2009). There, modern soil formation is marginal (Miehe, 1982; Saito & Tanaka, 2002), but extensive paleosol horizons set within a smooth, undulating topography suggest different conditions in the past. Importantly, this smooth paleo-landscape is dissected by canyons and gullies cutting into the underlying Neogene and Pleistocene sediments (Fort, 2014).

2.2. Methods

To assess erosion efficiency in the KG valley, we analyzed 6,346 suspended sediment concentration measurements from Lete, where the KG exits the upper valley, in 2011, 2012, 2015, and 2016, and downstream at Mirmi from 2006 to 2015.

We used SPOT multispectral imagery to distinguish the smooth paleo-landscape and badlands.

Lipid biomarkers were extracted from 27 oven-dried paleosol samples, 28 soil and 10 plant samples from 36 locations throughout the KG valley. The aliphatic fraction containing leaf wax *n*-alkanes was analyzed for compound-specific hydrogen isotope ratios (expressed as δD values) using a Delta-V-Plus Isotope Ratio Mass Spectrometer (Thermo Fisher Scientific) coupled to a Trace GC 1310 and for carbon isotope ratios ($\delta^{13}\text{C}$) on a Delta-V-Plus Isotope Ratio Mass Spectrometer coupled to an Agilent 7890 GC. δD ($\delta^{13}\text{C}$) values were normalized to the VSMOW (VPDB) scale using Schimmelmann's (Indiana University) *n*-alkane standard mix A6. For comparison, surface water δD values from the KG valley (elevation range 470 to 4,000 m; from 2013 and 2015) were analyzed using a Picarro Cavity Ringdown Spectrometer L2140-I and a Finnigan-MAT Delta-S Mass Spectrometer.

We used end-member modeling analysis (Dietze & Dietze, 2019) on 95 measured grain-size distributions to constrain the provenance of soil parent material.

Eight paleosol samples were analyzed for palynological information at Heidelberg University, Germany.

Thirteen paleosol samples and eight charcoal samples were radiocarbon dated at the Poznań AMS Radiocarbon Laboratory, Poland. Five samples were dated at the Netherlands Centre for Luminescence Dating at Wageningen University using Optically Stimulated Luminescence (OSL).

Further technical information on our methods is provided in Supporting Information S1.

3. Results and Discussion

3.1. Modern Landscape and Erosion Rates

Badlands and degraded soils occupy about half of the upper KG valley, above Chele (Figures 1b and S4), extending well beyond the actively incising channel network of the KG river (Figures S1–S3 and Text S2). Based on our hydrometric measurements, the badlands undergo fast erosion (Figure 1d), adding significantly to any sediment mobilized from within the channel network. At Lete, river suspended sediment concentrations are up to 2 orders of magnitude higher for a given water discharge than farther downstream, where river flow is dominated by High Himalayan drainage (Figures 1a and 1d). Despite low precipitation rates, <250 mm/year, and discharges from the upper valley rarely exceeding 100 m³/s, the modern erosion rate is 1 mm/year (Struck et al., 2015). The high sediment yield per unit of discharge from the upper catchment (Figure 1d, inset) suggests that precipitation can mobilize highly erodible materials poorly protected by the sparse vegetation resulting in a ~5 times higher erosion efficiency in the upper KG valley than in the High Himalayan part of the catchment (Figures 1a and 1d).

3.2. Chronology and Reconstruction of Paleo-landscape Dynamics

Remnants of a smooth, hilly paleo-landscape cover about 40% of the upper KG valley (Figure S5) extending north from Jomsom (Saito & Tanaka, 2002) to the drainage divide (Figures 1b and S1). Well-preserved paleosol horizons and sequences are present within this landscape, suggesting a significant period of geomorphic stability. These paleosols are typically covered by younger colluvium or loess or uncovered as relict soils or eroding soil remnants (Figure S2 and Table S2). They are, predominantly, <1 m thick Kastanozems (IUSS

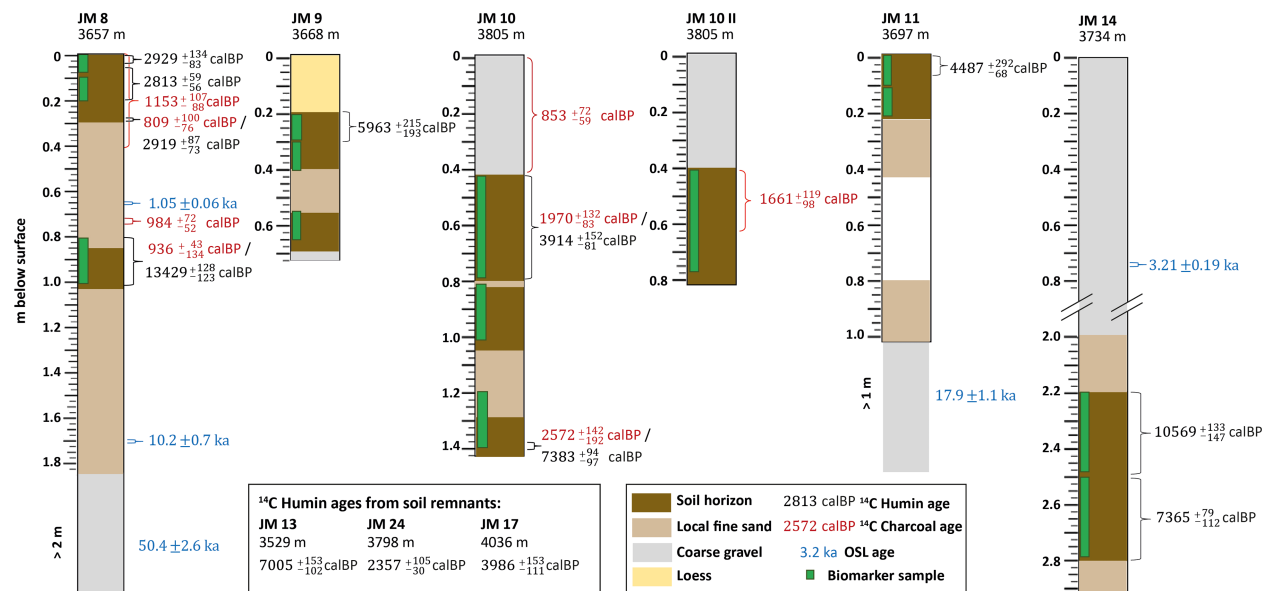


Figure 2. Overview of sampled paleosol sections (locations see Figures 1b and S1) with ¹⁴C humin fraction and charcoal ages and single-grain feldspar luminescence ages. ¹⁴C humin fraction ages from soil remnants elsewhere are shown in box.

Working Group WRB, 2015) with a mean total organic carbon content of $0.8 \pm 0.3\%$. End-member modeling analysis of grain size data (Figures S6 and S7) from 26 paleosol samples indicates that $85 \pm 12\%$ of the clastic parent material was delivered by wind or surface runoff from proximal sources (Text S4). The total organic carbon content covaries with the abundance of locally reworked sediment (Text S4), suggesting in situ organic matter production in an environment with ongoing deposition of fine clastic sediments. The local balance of these processes may have determined the location and timing of paleosol formation.

To constrain soil and landscape ages, we have measured the ¹⁴C content in soil organic matter and charcoal and used single-grain feldspar OSL. The timing of active paleosol formation was approximated using ¹⁴C measurements on residual soil organic matter, consisting of humins, mainly aliphatic hydrocarbons (Hayes et al., 2017), including leaf wax biomarkers. Paleosol humin ¹⁴C ages represent the time since soil formation ceased plus the accumulation time of the humins (Scharpenseel & Schiffman, 1977). To estimate the mean accumulation time of the humin fraction, we measured ¹⁴C ages at 5–30 cm depth in actively forming soils at two locations (JM05 and JM06) along the vegetated fringes of the upper KG valley (Figures 1 and S2), yielding ages of 599_{-55}^{+55} and $1,000_{-37}^{+52}$ cal. BP, respectively. We assume that the average of these ages, 800_{-240}^{+252} years, represents the local mean accumulation time of soil humins. This timespan is relatively long, as expected for semiarid environments with a slow carbon turnover (Schimel et al., 1994). Hence, we expect that paleosols contain humins with an age range of 1.6 ± 0.5 Kyr (2 times the mean accumulation time) and assign this range to the ¹⁴C humin ages when dating paleosol horizons and interpreting their pollen and biomarker content. Thirteen ¹⁴C paleosol humin ages from locations throughout the upper KG valley are evenly distributed from $13,429_{-342}^{+128}$ to $2,357_{-35}^{+105}$ cal. BP (Figure 2 and Table S3). Therefore, we infer that soil formation started at the end of the last glacial period, significantly earlier than previous constraints from the region (6.1–4.5 ka) (Saijo & Tanaka, 2002), and persisted during most of the Holocene. Considering the youngest dated paleosol ($2,357_{-35}^{+105}$ cal. BP) and including the 1.6 ± 0.5 Kyr humin age range, the youngest permitted age of soil formation in the main valley is around 1.6 ka.

We identified macroscopic charcoal with ¹⁴C ages ranging from $2,572_{-106}^{+129}$ to 809_{-65}^{+91} cal. BP ($n = 8$) in paleosols near Lo Manthang (Figure 2). Where available, charcoal ages are younger than the humin fraction of a given soil (see Figure 2). We assume that bioturbation has caused downward admixture of charcoal from near the surface into existing soil profiles (Carcaillet, 2001) (Text S5 and Figure S9). Hence, charcoal ¹⁴C ages were not used to infer paleosol ages but are instead thought to represent the timing of fire in the landscape.

Additional age constraints come from single-grain feldspar OSL (Reimann et al., 2012, 2017) ages for five sediment samples (Table S4). These ages represent the timing of the last exposure of sand grains at the surface. Typically, this is a depositional age, but bioturbation may cause the subsequent downward transport of daylight exposed particles into the underlying profile (Bateman et al., 2003). Two samples taken from coarse material at the base of profiles JM8 and JM11 date the deposition of the Pleistocene alluvial substrate to 50.4 ± 2.6 and 17.9 ± 1.1 ka (Figures 2 and S8). A coarse colluvial deposit on top of JM14, likely originated from a steep erosional hollow upslope, was dated to 3.2 ± 0.2 ka, indicating localized erosion at that time. Two luminescence samples taken from sands below paleosols in Section JM8 were affected by extensive bioturbation. We interpret their OSL ages to represent the end of active vertical mixing, that is, bioturbation, in the overlying soil horizons. The end of bioturbation in the younger paleosol of JM8 was dated to 1.05 ± 0.06 ka.

Taken together, we interpret the full chronological data set to reflect progressive deposition of locally derived sand, accompanied by persistent soil formation since the early Holocene, on top of Pleistocene alluvial substrate or older formations. These processes gave rise to a smooth, soil-covered landscape. Localized erosion and redeposition of coarser materials may have started around 3.2 ka, fires occurred regularly since at least 2.6 ka, and active soil formation ceased around 1.6 ka. We infer that the transformation into the present badland landscape has occurred since then.

3.3. Vegetation

Reduction of vegetation cover may have played an important role in the desertification and erosion of the upper KG landscape. Vegetation retains rainwater, modulates groundwater recharge, binds surface materials, and impedes surface runoff and sediment transport (Gyssels et al., 2005). KG paleosol pollen inventories indicate that an ensemble of nonarboreal steppe plants with abundant Asteraceae, Chenopodiaceae, and Poaceae dominated the region since the early Holocene, without significant tree cover or major compositional changes (Figure S10 and Text S6). The abundance of pollen in our samples systematically increased over time, peaking at ~ 4 ka (Figure 3a). However, by ~ 2.8 ka, a significant decline had started, suggesting a decrease in vegetation cover (Figure 3a), which may have facilitated a change toward the present erosive conditions. Potential drivers could have been overgrazing associated with human settlement and/or aridification through a decrease of water vapor flux across the Himalayas. Below, we consider both possibilities.

3.4. Human Impact

Today, rangeland degradation by traditional livestock husbandry occurs around Ghiling (Figure 1b) (Paudel & Andersen, 2010), even with a low population density of <5 inhabitants per km^2 (Fort, 2014). Tree harvesting has been suggested to have caused the decline of pine forest around 5.4 ka in Muktinath, in a slightly wetter side valley south of our study area (Figure 1b and Table S1) (Miehe et al., 2009). Nearby finds of charcoal dated to 4.5–5.7 ka indicate occurrence of fire (Saijo & Tanaka, 2002) attributed to human activity rather than lightning (Miehe et al., 2009). Archeological evidence from the upper KG valley (Figure 1b) indicates settlement from 3 ka (Simons et al., 1994), with agriculture and grazing livestock from 3.0 and 2.2 ka (Knörzer, 2000; von den Driesch et al., 2000). Our charcoal ^{14}C ages from near Lo Manthang suggest human land use from ~ 2.6 ka. Taken together, these observations indicate that human presence in this region during the last 3 Kyr and likely since around 5 ka has impacted the landscape through grazing and burning of woody vegetation (Figure 3a).

3.5. Past Hydroclimatic Change

Precipitation has also been identified as a limiting factor for the shrubland vegetation cover around Ghiling (Paudel & Andersen, 2010). The ISM domain was generally wetter in the early to mid-Holocene followed by a drying trend starting around 8–6 ka (Contreras-Rosales et al., 2014). The timing and local expression of this change varies across the Indian subcontinent (Prasad et al., 2014) and Tibet (Cai et al., 2012). To our knowledge, no local hydroclimatic record exists from the KG valley. Here we use hydrogen isotope ratios from the leaf wax $n\text{C}_{29}$ -alkane of higher plants ($\delta\text{D}_{\text{wax}}$) preserved in paleosols, as a proxy for the hydroclimatic conditions during soil formation (Sachse et al., 2012).

$\delta\text{D}_{\text{wax}}$ values in our paleosol samples (3,500–4,100 m asl., $13,429_{-76}^{+40}$ to $2,357_{-22}^{+46}$ cal. BP, $n = 24$) range from $-214\text{\textperthousand}$ to $-236\text{\textperthousand}$ (Figure 4a and Table S6). These values are offset by $-40 \pm 6\text{\textperthousand}$ from $\delta\text{D}_{\text{wax}}$ values of

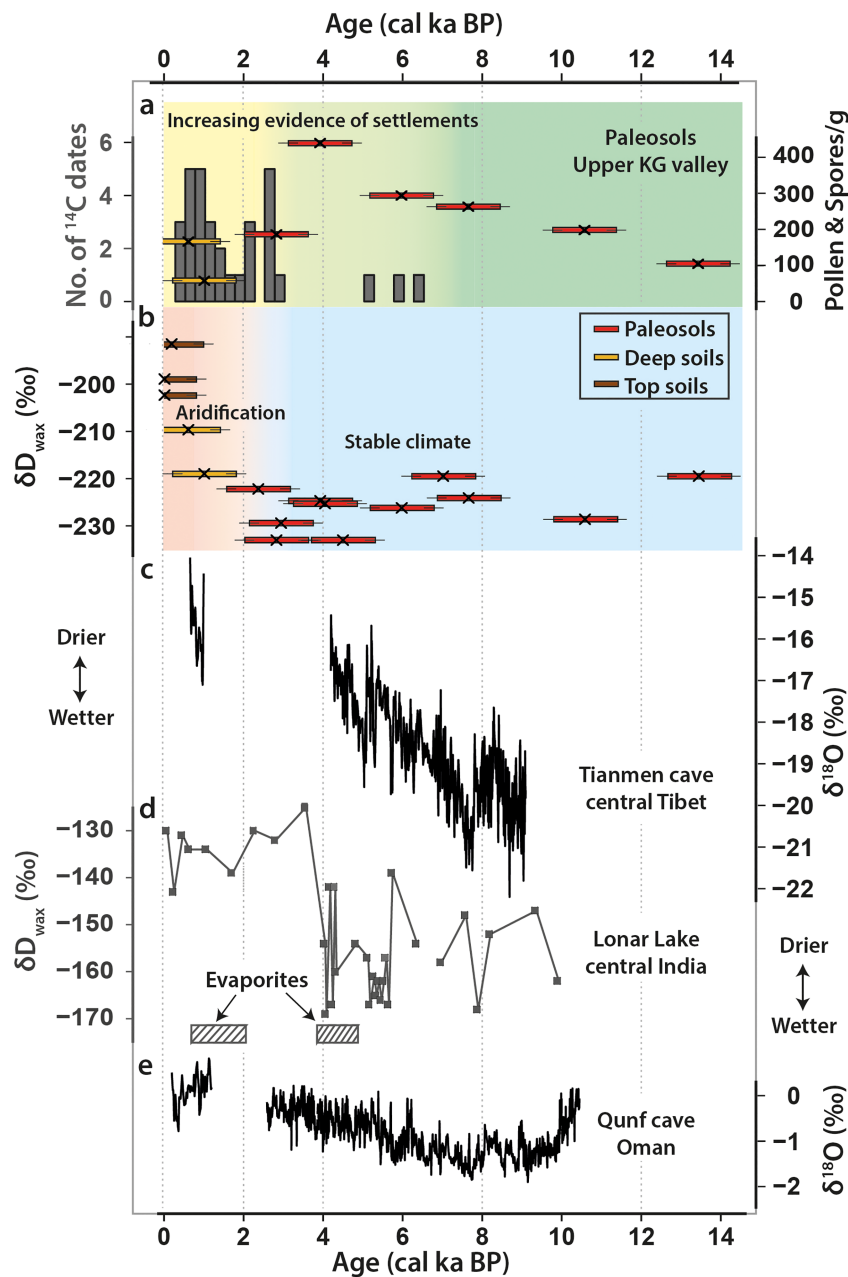


Figure 3. Paleosol data from the upper KG valley and Holocene climate records from the wider ISM region. (a) Histogram of ^{14}C -dated archeological and charcoal samples (gray) in the upper KG valley (Saijo & Tanaka, 2002; Simons et al., 1994) and this study (left y axis) and humin fraction ^{14}C ages (x) with integration time of 1.6 ± 0.5 Kyr versus summed pollen and spores concentrations for paleosols (red) and deep soils (yellow) (right y axis). (b) Humin fraction ^{14}C ages (x) with integration time of 1.6 ± 0.5 Kyr versus δD for paleosols (red), deep soils (yellow), and modern topsoils (brown). (c) $\delta^{18}\text{O}$ speleothem record from Tianmen cave, central Tibet (Cai et al., 2012). (d) δD_{wax} values and occurrence of Galussite crystals in Lonar Lake, Central India (Prasad et al., 2014; Sarkar et al., 2015). (e) $\delta^{18}\text{O}$ speleothem record from Qunf cave, Oman (Fleitmann et al., 2003).

modern *Caragana gerardiana* leaves sampled at the paleosol sites ($n = 10$, Figure 4b). Moreover, paleosol δD_{wax} values are generally more negative than modern topsoils sampled in the valley between 1,000 and 5,000 m asl ($-175\text{\textperthousand}$ to $-221\text{\textperthousand}$, $n = 17$, Figure 4a and Table S5). Modern topsoil δD_{wax} values show a typical increasing D depletion toward higher altitudes (Jia et al., 2008). In the altitude range of our paleosol samples, the offset of δD_{wax} values between paleosols and actively developing topsoils ($n = 3$) in the lateral valley fringe is $-36 \pm 4\text{\textperthousand}$ (Figures 1 and 3b). In our samples ($n = 3$) from deeper horizons of

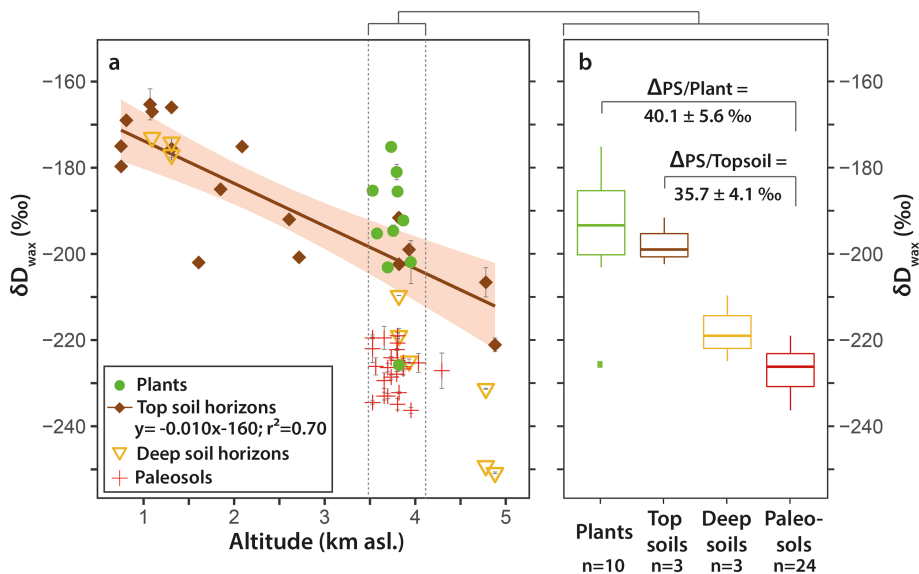


Figure 4. (a) δD_{wax} values for $n\text{-C}_{29}$ from modern plants (*Caragana gerardiana*) and topsoils, deeper soils, and paleosols plotted against sampling altitude; confidence interval around regression at 95%. (b) Box and whisker plots showing distribution of δD_{wax} values among different sample types from 3,500 to 4,200 m asl. $\Delta_{PS}/Plant$ denotes offset between paleosols and *Caragana gerardiana* and $\Delta_{PS}/Topsoil$ between paleosols and active topsoils. Boxes extend to first and third quartile and whiskers to extreme values within 1.5 interquartile range.

these modern soils in the lower KG valley (1,000–1,500 m asl), where a young ^{14}C bulk age of 42 years indicates fast organic matter overturning, δD_{wax} values are close to the overlying topsoils (Figure 4a). However, δD_{wax} values for deeper soil horizons are offset from topsoils by $-33 \pm 12\text{ ‰}$ in the upper valley (>4,500 m asl.), where humin fraction ^{14}C ages from 599 to 2,231 cal. BP ($n = 3$) suggest slower soil formation and carbon turnover. These findings indicate that the hydroclimate of the upper KG valley was wetter during the time of soil formation, followed by a change to drier conditions. Changes in vegetation type were minor according to our pollen data and cannot explain the observed isotopic shift (Figure S12 and Text S6).

Instead, we identify two mechanisms related to late Holocene aridification. First, the isotopic composition of ISM precipitation, the principal moisture source in the upper KG valley, is inversely correlated with the amount of precipitation in the tropics (Dansgaard, 1964) and imprinted on plant source waters in the Himalayas (Meese et al., 2018). Modeling suggests that a 50% decrease in ISM intensity between the middle and late Holocene has resulted in a 1.5‰ increase in precipitation $\delta^{18}\text{O}$ values or 12‰ in δD (LeGrande & Schmidt, 2009). Therefore, more negative paleosol δD_{wax} values likely indicate substantially wetter conditions during soil formation before 1.6 ka. However, even assuming an amplified response in the KG valley, it is unlikely that the full $36 \pm 4\text{ ‰}$ difference in δD_{wax} of paleosols and modern topsoils and vegetation arises from a shift in source water δD .

Second, leaf and soil water evaporative enrichment influences δD_{wax} especially under low relative humidity (rH), resulting in amplification of δD_{wax} changes (Kahmen et al., 2013; Kahmen et al., 2013). A Craig-Gordon based plant physiological model (Craig & Gordon, 1965; Kahmen et al., 2011; Kahmen, Hoffmann, et al., 2013; Rach et al., 2017) estimating leaf water isotope enrichment as a function of rH indicates that a 20% decrease in rH can result in a $16.2 \pm 2.6\text{ ‰}$ increase in δD_{wax} in the KG valley (Text S6). The effect of evaporation on leaf water δD values due to current dry conditions in the valley, exacerbated by strong upvalley winds (Egger et al., 2000), can be seen in the 15‰ decrease in difference between δD values of plant source waters and modern topsoil δD_{wax} values (apparent fractionation ϵ_{app}) toward the upper KG valley (Figure S11 and Text S6). We therefore suggest that the more negative mid-Holocene paleosol δD_{wax} values result from a more intense ISM combined with up to 20% higher relative humidity.

In summary, leaf wax isotopic evidence suggests that relatively stable, wetter conditions than today prevailed in the upper KG valley throughout the Holocene until around 2.4 ka (Figure 3b). Our data from

this interval show minor δD_{wax} variations, but the relatively long integration time of the soil samples (Schlesinger, 1990) may have eliminated any high frequency signals. We find no evidence of substantial aridification in the upper KG valley during the transition to a less intense ISM around 6–4 ka, a transition affecting many locations in the ISM domain (Cai et al., 2012; Fleitmann et al., 2003). In contrast, deeper regional aridification around 2 ka, reflected by desiccation of speleothem records from Oman (Fleitmann et al., 2003) and central Tibet (Cai et al., 2012), and evaporite deposition in Lonar Lake (Prasad et al., 2014) in the ISM core region, also impacted the upper KG valley (Figures 3b–3e). Both the mid-Holocene stability and the comparatively large amplitude of the δD_{wax} shift after ~2.4 ka suggest that local conditions, potentially the valley topography and its role in funneling air masses from India to the Tibetan Plateau (Egger et al., 2000), modulated the hydroclimate of this trans-Himalayan valley.

4. Conclusions and Implications

4.1. Combined Effect of Human Pressure and Aridification

Our findings suggest that geomorphic stability during the early and middle Holocene coincided with stable hydroclimatic conditions, permitting prolonged soil formation throughout the upper KG valley. Increasing human presence from 3 ka onward (Simons et al., 1994) coincided with a drastic reduction of pollen in paleosols, indicating a decrease of vegetation cover at this time, potentially caused by grazing and priming the landscape for desertification. Drier conditions after ~2.4 ka likely further compromised vegetation growth, finally leading to cessation of soil formation after ~1.6 ka and wholesale landscape desiccation. Could land use alone have been able to tip the landscape into rapid erosion or was the additional climatic impact required? Large tracts of soil-covered landscape are preserved in the KG valley south of Chele (Figures 1b and S5), where the average precipitation exceeds 200 mm/year, even though the population density is higher, implying that moisture is the dominant control. The recorded aridification, with precipitation dropping below the current amounts at Chele and an attendant relative humidity drop of about 20%, has moved the eco-geomorphic system across a threshold and into full degradation around 1.6 ka, after human impact lowered its resilience.

4.2. Implications

Today, the devegetated upper KG landscape is prone to fast erosion due to surface runoff and carving of gullies. Current catchment-average erosion rates of 1 m/Kyr (Struck et al., 2015) are enough to excavate the paleosols on this time scale. The effects are irreversible because the newly formed badland topography does not permit effective revegetation and soil formation. A future precipitation increase might therefore result in a further increase in erosion and soil export. Where this tipping point has been crossed, vital landscape services may be lost on millennial time scales, compromising the ability of people to maintain a foothold in this dryland. Extrapolating the conditions that caused the KG tipping point, areas at risk under moderate human impact may lie within the 200 mm/year isohyet. Finally, our observations show that large-scale climate trends, such as changes in ISM strength, can have locally differentiated expressions, warranting a focus on landscape-scale systems and their thresholds.

Funding

This work was supported by the Helmholtz Impuls und Vernetzung Fond. Field work was supported by the GFZ expedition funding in 2014 and 2016.

Authors Contributions

J. M., N. H., D. S., and C. A. designed the study. J. M., N. H., D. S., C. A., K. C., S. B., C. S., M. D., B. A., A. V. H., T. R., and A. K. collected and/or processed samples and analyzed data. J. M., N. H., and D. S. wrote the manuscript with contributions from all other coauthors.

Competing Interests

The authors declare no competing financial interests.

Data and Materials Availability

This manuscript is accompanied by Supporting Information S1. The data used in this study are available under the following reference:

Menges, Johanna; Hovius, Niels; Andermann, Christoff; Dietze, Michael; Swoboda, Charlie; Cook, Kristen; Adhikari, Basanta; Vieth-Hillebrand, Andrea; Bonnet, Stephane; Reimann, Tony; Koutsodendris, Andreas; Sachse, Dirk (2019): Paleosol-derived data used for the reconstruction of environmental conditions during the Holocene in the upper part of the Kali Gandaki valley, Central Nepal. GFZ Data Services. <http://doi.org/10.5880/GFZ.4.6.2019.001>

Acknowledgments

We thank Maarten Lupker (ETH Zurich) and Camilla Brunello (GFZ Potsdam) for collecting some of the samples; Nathalie Benoit, Stefan Liening, and Caroline Zorn for help during the lab processing of suspended sediments and soil samples; Martin Struck for sediment data analysis; Birgit Plessen and Petra Meier (GFZ Potsdam) for TOC measurements; Hanno Meyer (AWI Potsdam stable isotope laboratory) for providing some of the stable isotope measurements; Alice Versendaal (NCL) for technical support of the luminescence dating analyses; and Oliver Kern (Heidelberg University) for the palynological processing. Acquisition of SPOT images (SB) was supported by public funds received in the framework of GEOSUD, a project (ANR-10-EQPX-20) of the program “Investissements d’Avenir” managed by the French National Research Agency. We further thank Doug Burbank and one anonymous reviewer for helpful comments which substantially improved the manuscript.

References

- Adhikari, B. R., & Wagreich, M. (2011). Facies analysis and basin architecture of the Thakkola-Mustang Graben (Neogene-Quaternary), central Nepal Himalaya. *Austrian Journal of Earth Science*, 104(1), 66–80.
- Aldenderfer, M., & Eng, J. T. (2016). Death and burial among two ancient high-altitude communities of Nepal in A companion to South Asia in the past. In G. R. Schug & S. R. Walimbe (Eds.), *A companion to South Asia in the past* (pp. 1–564). West Sussex, UK: John Wiley & Sons, Inc. <https://doi.org/10.1002/9781119055280>
- Bateman, M. D., Frederick, C. D., Jaiswal, M. K., & Singhvi, A. K. (2003). Investigations into the potential effects of pedoturbation on luminescence dating. *Quaternary Science Reviews*, 22(10–13), 1169–1176. [https://doi.org/10.1016/S0277-3791\(03\)00019-2](https://doi.org/10.1016/S0277-3791(03)00019-2)
- Bookhagen, B., & Burbank, D. W. (2010). Toward a complete Himalayan hydrological budget: Spatiotemporal distribution of snowmelt and rainfall and their impact on river discharge. *Journal of Geophysical Research*, 115, F03019. <https://doi.org/10.1029/2009JF001426>
- Cai, Y., Zhang, H., Cheng, H., An, Z., Lawrence Edwards, R., Wang, X., et al. (2012). The Holocene Indian monsoon variability over the southern Tibetan Plateau and its teleconnections. *Earth and Planetary Science Letters*, 335–336, 135–144. <https://doi.org/10.1016/j.epsl.2012.04.035>
- Carcaillet, C. (2001). Are Holocene wood-charcoal fragments stratified in alpine and subalpine soils? Evidence from the Alps based on AMS14C dates. *Holocene*, 11(2), 231–242. <https://doi.org/10.1191/095968301674071040>
- Contreras-Rosales, L. A., Jennerjahn, T., Tharammal, T., Meyer, V., Lückge, A., Paul, A., & Schefuß, E. (2014). Evolution of the Indian Summer Monsoon and terrestrial vegetation in the Bengal region during the past 18ka. *Quaternary Science Reviews*, 102, 133–148. <https://doi.org/10.1016/j.quascirev.2014.08.010>
- Craig, H., & Gordon, I. (1965). Deuterium and oxygen 18 variations in the ocean and the marine atmosphere. In E. Tongiorgi (Ed.), *Stable isotopes in oceanographic studies and paleotemperatures* (pp. 9–130). Consiglio Nazionale delle Ricerche: Spoleto. <https://doi.org/10.1109/ISSRE.1993.624301>
- Cui, X., & Graf, H. (2009). Recent land cover changes on the Tibetan Plateau: A review. *Climatic Change*, 94, 47–61. <https://doi.org/10.1007/s10584-009-9556-8>
- Dansgaard, W. (1964). Stable isotopes in precipitation. *Tellus*, 16(4), 436–468. <https://doi.org/10.3402/tellusa.v16i4.8993>
- Dietze, E., & Dietze, M. (2019). Grain-size distribution unmixing using the R package EMMAgeo. *E&G Quaternary Science Journal*, 68(1), 29–46. <https://doi.org/10.5194/egqsj-68-29-2019>
- D’Odorico, P., Bhattachan, A., Davis, K. F., Ravi, S., & Runyan, C. W. (2013). Global desertification: Drivers and feedbacks. *Advances in Water Resources*, 51(October 2017), 326–344. <https://doi.org/10.1016/j.advwatres.2012.01.013>
- Egger, J., Bajracharya, S., Egger, U., Heinrich, R., Reuder, J., Shayka, P., et al. (2000). Diurnal winds in the Himalayan Kali Gandaki Valley. Part I: Observations. *Monthly Weather Review*, 128(4), 1106–1122. [https://doi.org/10.1175/1520-0493\(2000\)128<1106:DWITHK>2.0.CO;2](https://doi.org/10.1175/1520-0493(2000)128<1106:DWITHK>2.0.CO;2)
- Fleitmann, D., Burns, S. J., Mudelsee, M., Neff, U., Kramers, J., Mangini, A., & Matter, A. (2003). Holocene forcing of the Indian monsoon recorded in a stalagmite from Southern Oman. *Science*, 300(June), 1737–1740.
- Fort, M. (2014). Natural hazards versus climate change and their potential impacts in the dry, northern Himalayas: Focus on the upper Kali Gandaki (Mustang District, Nepal). *Environmental Earth Sciences*, 73, 801–814. <https://doi.org/10.1007/s12665-014-3087-y>
- Fort, M., Freytet, P., & Colchen, M. (1982). Structural and sedimentological evolution of the Thakkola Mustang Graben (Nepal Himalayas). *Zeitschrift Fur Geomorphologic N.F.*, 42, 75–98.
- Garzzone, C. N., Quade, J., DeCelles, P. G., & English, N. B. (2000). Predicting paleoelevation of Tibet and the Himalaya from $\delta^{18}\text{O}$ vs. altitude gradients in meteoric water across the Nepal Himalaya. *Earth and Planetary Science Letters*, 183(1–2), 215–229. [https://doi.org/10.1016/S0012-821X\(00\)00252-1](https://doi.org/10.1016/S0012-821X(00)00252-1)
- Gyssels, G., Poesen, J., Bochet, E., & Li, Y. (2005). Impact of plant roots on the resistance of soils to erosion by water: a review. *Progress in Physical Geography: Earth and Environment*, 29(2), 189–217. <https://doi.org/10.1191/030913305pp443ra>
- Hayes, M. H. B., Mylrore, R., & Swift, R. S. (2017). Humin: Its composition and importance in soil organic matter. In D. L. Sparks (Ed.), *Advances in Agronomy*. Burlington: Elsevier Inc.
- IUSS Working Group WRB (2015). International soil classification system for naming soils and creating legends for soil maps. World Reference Base for Soil Resources 2014 Update 2015 (Vol. 106). Rome: FAO. <https://doi.org/10.1017/S0014479706394902>
- Jia, G., Wei, K., Chen, F., & Peng, P. (2008). Soil n-alkane δD vs. altitude gradients along Mount Gongga, China. *Geochimica et Cosmochimica Acta*, 72(21), 5165–5174. <https://doi.org/10.1016/j.gca.2008.08.004>
- Kahmen, A., Hoffmann, B., Schefuß, E., Arndt, S. K., Cernusak, L. A., West, J. B., & Sachse, D. (2013). Leaf water deuterium enrichment shapes leaf wax n-alkane δD values of angiosperm plants II: Observational evidence and global implications. *Geochimica et Cosmochimica Acta*, 111, 50–63. <https://doi.org/10.1016/j.gca.2012.09.004>
- Kahmen, A., Sachse, D., Arndt, S. K., Tu, K. P., Farrington, H., & Vitousek, P. M. (2011). Cellulose $\delta^{18}\text{O}$ is an index of leaf-to-air vapor pressure difference (VPD) in tropical plants. *Proceedings of the National Academy of Sciences*, 108(5), 1981–1986. <https://doi.org/10.1073/pnas.1018906108>
- Kahmen, A., Schefuß, E., & Sachse, D. (2013). Leaf water deuterium enrichment shapes leaf wax n-alkane δD values of angiosperm plants I: Experimental evidence and mechanistic insights. *Geochimica et Cosmochimica Acta*, 111, 39–49. <https://doi.org/10.1016/j.gca.2012.09.003>

- Knörzer, K.-H. (2000). 3000 years of agriculture in a valley of the High Himalayas. *Vegetation History and Archaeobotany*, 9(4), 219–222. <https://doi.org/10.1007/BF01294636>
- Kriechbaum, M. (2002). Flora, Vegetation und Landnutzung des Muktinath-Tales (Mustang, Nepal) als Beziehungsmuster von naturräumlicher Ausstattung und menschlicher Gestaltung im Zentralhimalaya. *Dissertationes Botanicae*, 369.
- LeGrande, A. N., & Schmidt, G. A. (2009). Sources of Holocene variability of oxygen isotopes in paleoclimate archives. *Climate of the Past*, 5(3), 441–455. <https://doi.org/10.5194/cp-5-441-2009>
- Meese, B., Bookhagen, B., Olen, S. M., Barthold, F., & Sachse, D. (2018). The effect of Indian summer monsoon rainfall on surface water δD values in the central Himalaya. *Hydrological Processes*, 32(24), 3662–3674. <https://doi.org/10.1002/hyp.13281>
- Meyer, M. C., Aldenderfer, M. S., Wang, Z., Hoffmann, D. L., Dahl, J. A., Degering, D., et al. (2017). Permanent human occupation of the central Tibetan Plateau in the early Holocene. *Science*, 355(6320), 64–67. <https://doi.org/10.1126/science.aag0357>
- Miehe, G. (1982). Vegetationsgeographische Untersuchungen im Dhawalagiri- und Annapurna-Himalaya. *Dissertationes Botanicae*, 66.
- Miehe, G., Miehe, S., Böhner, J., Kaiser, K., Hensen, I., Madsen, D., et al. (2014). How old is the human footprint in the world's largest alpine ecosystem? A review of multiproxy records from the Tibetan Plateau from the ecologists' viewpoint. *Quaternary Science Reviews*, 86, 190–209. <https://doi.org/10.1016/j.quascirev.2013.12.004>
- Miehe, G., Miehe, S., & Schlüter, F. (2009). Early human impact in the forest ecotone of southern High Asia (Hindu Kush, Himalaya). *Quaternary Research*, 71(3), 255–265. <https://doi.org/10.1016/j.yqres.2009.02.004>
- Millennium Ecosystem Assessment (2005). Ecosystems and human well-being: Desertification synthesis. Ecosystems and human well-being.
- Paudel, K. P., & Andersen, P. (2010). Assessing rangeland degradation using multi temporal satellite images and grazing pressure surface model in Upper Mustang, Trans Himalaya, Nepal. *Remote Sensing of Environment*, 114(8), 1845–1855. <https://doi.org/10.1016/j.rse.2010.03.011>
- Prasad, S., Anoop, A., Riedel, N., Sarkar, S., Menzel, P., Basavaiah, N., et al. (2014). Prolonged monsoon droughts and links to Indo-Pacific warm pool: A Holocene record from Lonar Lake, central India. *Earth and Planetary Science Letters*, 391, 171–182. <https://doi.org/10.1016/j.epsl.2014.01.043>
- Rach, O., Kahmen, A., Brauer, A., & Sachse, D. (2017). A dual-biomarker approach for quantification of changes in relative humidity from sedimentary lipid D/H ratios. *Climate of the Past*, 13, 741–757.
- Reimann, T., Román-Sánchez, A., Vanwallagem, T., & Wallinga, J. (2017). Getting a grip on soil reworking—Single-grain feldspar luminescence as a novel tool to quantify soil reworking rates. *Quaternary Geochronology*, 42, 1–14. <https://doi.org/10.1016/j.quageo.2017.07.002>
- Reimann, T., Thomsen, K. J., Jain, M., Murray, A. S., & Frechen, M. (2012). Single-grain dating of young sediments using the pIRIR signal from feldspar. *Quaternary Geochronology*, 11, 28–41. <https://doi.org/10.1016/j.quageo.2012.04.016>
- Reynolds, J. F., Smith, D. M. S., Lambin, E. F., Turner, B. L., Mortimore, M., Batterbury, S. P. J., et al. (2007). Global desertification: Building a science for dryland development. *Science*, 316(5826), 847–851. <https://doi.org/10.1126/science.1131634>
- Sachse, D., Billault, I., Bowen, G. J., Chikaraishi, Y., Dawson, T. E., Feakins, S. J., et al. (2012). Molecular paleohydrology: Interpreting the hydrogen-isotopic composition of lipid biomarkers from photosynthesizing organisms. *Annual Review of Earth and Planetary Sciences*, 40(1), 221–249. <https://doi.org/10.1146/annurev-earth-042711-105535>
- Saijo, K., & Tanaka, S. (2002). Paleosols of middle Holocene age in the Thakkhola basin, central Nepal, and their paleoclimatic significance. *Journal of Asian Earth Sciences*, 21(3), 323–329. [https://doi.org/10.1016/S1367-9120\(02\)00079-2](https://doi.org/10.1016/S1367-9120(02)00079-2)
- Sarkar, S., Prasad, S., Wilkes, H., Riedel, N., Stebich, M., Basavaiah, N., & Sachse, D. (2015). Monsoon source shifts during the drying mid-Holocene: Biomarker isotope based evidence from the core ‘monsoon zone’ (CMZ) of India. *Quaternary Science Reviews*, 123, 144–157. <https://doi.org/10.1016/j.quascirev.2015.06.020>
- Scharpenseel, H. W., & Schiffman, H. (1977). Radiocarbon dating of soils, a review. *Z. Pflanzernernaehr. Bodenkdl.*, 140(1977), 159–174. <https://doi.org/10.1002/jpln.19771400205>
- Scheffer, M., Carpenter, S., Foley, J. A., Folke, C., & Walker, B. (2001). Catastrophic shifts in ecosystems. *Nature*, 413(6856), 591–596. <https://doi.org/10.1038/35098000>
- Schimel, D. S., Braswell, B. H., Holland, E. A., McKeown, R., Ojima, D. S., Painter, T. H., et al. (1994). Climatic, edaphic, and biotic controls over storage and turnover of carbon in soils. *Global Biogeochemical Cycles*, 8(3), 279–293. <https://doi.org/10.1029/94GB00993>
- Schlesinger, W. H. (1990). Evidence from chronosequence studies for a low carbon-storage potential of soils. *Nature*, 348(6298), 232–234. <https://doi.org/10.1038/348232a0>
- Shen, C., Liu, K. B., Morrill, C., Overpeck, J. T., Peng, J., & Tang, L. (2008). Ecotone shift and major droughts during the mid-late Holocene in the central Tibetan Plateau. *Ecology*, 89(4), 1079–1088. <https://doi.org/10.1890/06-2016.1>
- Simons, A., Schon, W., & Shrestha, S. S. (1994). Preliminary Report on the 1992 Campaign of the Team of the Institute of Prehistory, University of Cologne. *Ancient Nepal, Journal of the Department of Archaeology*, 136, 51–75.
- Struck, M., Andermann, C., Hovius, N., Korup, O., Turowski, J. M., Bista, R., et al. (2015). Monsoonal hillslope processes determine grain size-specific suspended sediment fluxes in a trans-Himalayan river. *Geophysical Research Letters*, 42, 2302–2308. <https://doi.org/10.1002/2015GL063360>
- UNCCD (1994). United Nations convention to combat desertification in countries experiencing serious drought and/or desertification, particularly in Africa. United Nations (Vol. A/AC). Paris.
- von den Driesch, A., Manhart, H., & Schmitt, B. (2000). Archäozoologische Untersuchungen in der mittelalterlichen Siedlung von Khyinga-Khalun, Distrikt Mustang/Nepal. *Beiträge Zur Allgemeinen Und Vergleichenden Archäologie*, 20, 45–108.

References From the Supporting Information

- Aitken, M. J. (1985). *Thermoluminescence dating*. London: Academic Press. <https://doi.org/10.1016/B978-044450487-6/50052-3>
- Andermann, C., Longuevergne, L., Bonnet, S., Crave, A., Davy, P., & Gloaguen, R. (2012). Impact of transient groundwater storage on the discharge of Himalayan rivers. *Nature Geoscience*, 5(2), 127–132. <https://doi.org/10.1038/ngeo1356>
- Bai, Y., Fang, X., Jia, G., Sun, J., Wen, R., & Ye, Y. (2015). Different altitude effect of leaf wax n-alkane δD values in surface soils along two vapor transport pathways, southeastern Tibetan Plateau. *Geochimica et Cosmochimica Acta*, 170, 94–107. <https://doi.org/10.1016/j.gca.2015.08.016>
- Bötter-Jensen, L., Andersen, C. E., Duller, G. A. T., & Murray, A. S. (2003). Developments in radiation, stimulation and observation facilities in luminescence measurements. *Radiation Measurements*, 37(4–5), 535–541. [https://doi.org/10.1016/S1350-4487\(03\)00020-9](https://doi.org/10.1016/S1350-4487(03)00020-9)

- Bush, R. T., & Mcinerney, F. A. (2013). Leaf wax n-alkane distributions in and across modern plants: Implications for paleoecology and chemotaxonomy. *Geochimica et Cosmochimica Acta*, 117, 161–179. <https://doi.org/10.1016/j.gca.2013.04.016>
- Cunningham, A. C., & Wallinga, J. (2012). Realizing the potential of fluvial archives using robust OSL chronologies. *Quaternary Geochronology*, 12, 98–106. <https://doi.org/10.1016/j.quageo.2012.05.007>
- Dietze, E., Hartmann, K., Diekmann, B., IJmker, J., Lehmkühl, F., Opitz, S., et al. (2012). An end-member algorithm for deciphering modern detrital processes from lake sediments of Lake Donggi Cona, NE Tibetan Plateau, China. *Sedimentary Geology*, 243–244, 169–180. <https://doi.org/10.1016/j.sedgeo.2011.09.014>
- Dietze, E., Maussion, F., Ahlborn, M., Diekmann, B., Hartmann, K., Henkel, K., et al. (2014). Sediment transport processes across the Tibetan Plateau inferred from robust grain-size end members in lake sediments. *Climate of the Past*, 10(1), 91–106. <https://doi.org/10.5194/cp-10-91-2014>
- Dietze, M., Dietze, E., Lomax, J., Fuchs, M., Kleber, A., & Wells, S. G. (2016). Environmental history recorded in aeolian deposits under stone pavements, Mojave Desert, USA. *Quaternary Research (United States)*, 85(1), 4–16. <https://doi.org/10.1016/j.yqres.2015.11.007>
- Duller, G. A. T. (2008). Single-grain optical dating of Quaternary sediments: Why aliquot size matters in luminescence dating. *Boreas*, 37(4), 589–612. <https://doi.org/10.1111/j.1502-3885.2008.00051.x>
- Feeakins, S. J. (2013). Pollen-corrected leaf wax D/H reconstructions of northeast African hydrological changes during the late Miocene. *Palaeogeography, Palaeoclimatology, Palaeoecology*, 374, 62–71. <https://doi.org/10.1016/j.palaeo.2013.01.004>
- Galbraith, R. F., Roberts, R. G., Laslett, G. M., Yoshida, H., & Olley, J. M. (1999). Optical dating of single and multiple grains of quartz from Jinmium rock shelter, northern Australia: Part I, experimental design and statistical models. *Archaeometry*, 2(FEBRUARY), 339–364. <https://doi.org/10.1111/j.1475-4754.1999.tb00987.x>
- Garcin, Y., Deschamps, P., Ménot, G., de Saulieu, G., Scheufuß, E., Sebag, D., et al. (2018). Early anthropogenic impact on Western Central African rainforests 2,600 y ago. *Proceedings of the National Academy of Sciences*, 115(13), 3261–3266. <https://doi.org/10.1073/pnas.1715336115>
- Garcin, Y., Scheufuß, E., Schwab, V. F., Garreta, V., Gleixner, G., Vincens, A., et al. (2014). Reconstructing C3 and C4 vegetation cover using n-alkane carbon isotope ratios in recent lake sediments from Cameroon, Western Central Africa. *Geochimica et Cosmochimica Acta*, 142, 482–500. <https://doi.org/10.1016/j.gca.2014.07.004>
- Guérin, G., Mercier, N., & Adamiec, G. (2011). Dose-rate conversion factors: Update. *Ancient TL*, 29(1), 5–8. <https://doi.org/10.7314/APJCP.2014.15.6.2523>
- Kars, R. H., Busschers, F. S., & Wallinga, J. (2012). Validating post IR-IRSL dating on K-feldspars through comparison with quartz OSL ages. *Quaternary Geochronology*, 12, 74–86. <https://doi.org/10.1016/j.quageo.2012.05.001>
- Madsen, A. T., Murray, A. S., Andersen, T. J., Pejrup, M., & Breuning-Madsen, H. (2005). Optically stimulated luminescence dating of young estuarine sediments: A comparison with 210Pb and 137Cs dating. *Marine Geology*, 214(1–3), 251–268. <https://doi.org/10.1016/j.margeo.2004.10.034>
- Mejdahl, V. (1979). Thermoluminescence dating: Beta-dose attenuation in quartz grains. *Archaeometry*, 21(1), 61–72.
- Menges, J., Hovius, N., Andermann, C., Dietze, M., Swoboda, C., Cook, K., et al. (2019). Paleosol-derived data used for the reconstruction of environmental conditions during the Holocene in the upper part of the Kali Gandaki valley, Central Nepal. GFZ Data Services. <https://doi.org/http://doi.org/10.5880/GFZ.4.6.2019.001>
- Meyer, H., Schönicke, L., Wand, U., Hubberten, H. W., & Friedrichsen, H. (2000). Isotope studies of hydrogen and oxygen in ground ice—Experiences with the equilibration technique. *Isotopes in Environmental and Health Studies*, 36(2), 133–149. <https://doi.org/10.1080/10256010008032939>
- Minze, S., & Reimer, P. J. (1993). Extended ^{14}C data base and revised CALIB 3.0 ^{14}C age calibration program. *Radiocarbon*, 35(1), 215–230.
- Pessenda, L. C. R., Gouveia, S. E. M., & Aravena, R. (2001). Radiocarbon dating of total soil organic matter and humin fraction and its comparison with ^{14}C ages of fossil charcoal. *Radiocarbon*, 43(Nr2B), 595–601.
- Prescott, J. R., & Hutton, J. T. (1994). Cosmic ray contributions to dose rates for luminescence and ESR dating: Large depths and long-term time variations. *Radiation Measurements*, 23(2–3), 497–500. [https://doi.org/10.1016/1350-4487\(94\)90086-8](https://doi.org/10.1016/1350-4487(94)90086-8)
- Preusser, F., Degering, D., Fuchs, M., Hilgers, A., Kadereit, A., Klasen, N., et al. (2008). Luminescence dating: Basics, methods and applications. *Eiszeitalter Und Gegenwart*, 57(1–2), 95–149.
- Rao, Z., Zhu, Z., Jia, G., Henderson, A. C. G., Xue, Q., & Wang, S. (2009). Compound specific δD values of long chain n-alkanes derived from terrestrial higher plants are indicative of the δD of meteoric waters: Evidence from surface soils in eastern China. *Organic Geochemistry*, 40(8), 922–930. <https://doi.org/10.1016/j.orggeochem.2009.04.011>
- Schwab, V. F., Garcin, Y., Sachse, D., Todou, G., Séne, O., Onana, J. M., et al. (2015). Effect of aridity on $\delta^{13}\text{C}$ and δD values of C3 plant- and C4 graminoid-derived leaf wax lipids from soils along an environmental gradient in Cameroon (Western Central Africa). *Organic Geochemistry*, 78(July), 99–109. <https://doi.org/10.1016/j.orggeochem.2014.09.007>
- Smedley, R. K., Duller, G. A. T., Pearce, N. J. G., & Roberts, H. M. (2012). Determining the K-content of single-grains of feldspar for luminescence dating. *Radiation Measurements*, 47(9), 790–796. <https://doi.org/10.1016/j.radmeas.2012.01.014>
- Tanner, B. R., Uhle, M. E., Mora, C. I., Kelley, J. T., Schuneman, P. J., Lane, C. S., & Allen, E. S. (2010). Comparison of bulk and compound-specific $\delta^{13}\text{C}$ analyses and determination of carbon sources to salt marsh sediments using n-alkane distributions (Maine, USA). *Estuarine, Coastal and Shelf Science*, 86(2), 283–291. <https://doi.org/10.1016/j.ecss.2009.11.023>
- Thomas, E. K., Huang, Y., Morrill, C., Zhao, J., Wegener, P., Clemens, S. C., et al. (2014). Abundant C4 plants on the Tibetan Plateau during the Lateglacial and early Holocene. *Quaternary Science Reviews*, 87, 24–33. <https://doi.org/10.1016/j.quascirev.2013.12.014>
- Thomsen, K. J., Murray, A. S., Jain, M., & Bøtter-Jensen, L. (2008). Laboratory fading rates of various luminescence signals from feldspar-rich sediment extracts. *Radiation Measurements*, 43(9–10), 1474–1486. <https://doi.org/10.1016/j.radmeas.2008.06.002>
- Trumbore, S. E. (2009). Radiocarbon and soil carbon dynamics. *Annual Review of Earth and Planetary Sciences*, 37(1), 47–66. <https://doi.org/10.1146/annurev.earth.36.031207.124300>
- Vandenbergh, J. (2013). Grain size of fine-grained windblown sediment: A powerful proxy for process identification. *Earth-Science Reviews*, 121, 18–30. <https://doi.org/10.1016/j.earscirev.2013.03.001>
- Wang, Y., Amundson, R., & Trumbore, S. E. (1996). Radiocarbon dating of soil organic matter. *Quaternary Research*, 45(3), 282–288. <https://doi.org/10.1006/qres.1996.0029>
- Wang, Y. V., Larsen, T., Leduc, G., Andersen, N., Blanz, T., & Schneider, R. R. (2013). What does leaf wax δD from a mixed C3/C4 vegetation region tell us? *Geochimica et Cosmochimica Acta*, 111, 128–139. <https://doi.org/10.1016/j.gca.2012.10.016>
- Weltje, G. J. (1997). End-member modeling of compositional data: Numerical-statistical algorithms for solving the explicit mixing problem. *Mathematical Geology*, 29(4), 503–549. <https://doi.org/10.1007/BF02775085>